

# Molecular-dynamics study of the local motion in a glass model for $\text{Rb}_{1-x}(\text{ND}_4)_x\text{D}_2\text{PO}_4$

Krzysztof Parlinski

*Institute of Nuclear Physics, 31-342 Cracow, Poland*

Hans Grimm

*Institut für Festkörperforschung, Kernforschungsanlage Jülich, D-5170 Jülich, Federal Republic of Germany*

(Received 8 June 1987)

A model with four protons and two randomly chosen effective rubidium and/or ammonium particles per unit cell has been studied by the molecular-dynamics method. The mixed system forms a structural glass below some freezing temperature. In the glassy state a pattern of ferroelectric and antiferroelectric quasipermanent clusters with random orientations exists. In addition, regions of active jump motion of protons are observed. Because of inequivalent proton environments, the square displacement and the average potential-energy fluctuations of individual protons are represented by broad, wide distributions. The same distributions in the paraelectric state of the mixed system and in the crystal are narrow. The spectra of elementary relaxation times for glassy and crystal systems have been calculated and compared. The results agree with the concept of a hierarchy of degrees of freedom.

## I. INTRODUCTION

Systems with randomly competing interactions forming structural glasses on lowering the temperatures are one of the most active subjects of statistical mechanics. The mixed system of ferroelectric  $\text{RbH}_2\text{PO}_4$  (RDP) and antiferroelectric  $\text{NH}_4\text{H}_2\text{PO}_4$  (ADP) has attracted considerable attention in this respect.  $\text{Rb}_{1-x}(\text{NH}_4)_x\text{H}_2\text{PO}_4$  (RADP) appears to be a perfectly random mixture of the constituents. In the intermediate range of concentration  $0.233 < x < 0.74$ , the built-in frustration of RADP prevents ordinary ferroelectric or antiferroelectric phase transitions and the disordered acid-proton sublattice freezes into a structural glass.

Peculiar properties of the RADP glassy state have been observed with a variety of experimental techniques, including dielectric dispersion,<sup>1-4</sup> Raman<sup>5</sup> and Brillouin<sup>6-9</sup> scattering, x-ray diffraction,<sup>10-16</sup> NMR,<sup>17,18</sup> optical birefringence,<sup>19</sup> and neutron scattering.<sup>20,21</sup> The x-ray and neutron measurements revealed diffuse scattering in the incommensurate position, which is a result of the coherent scattering from frozen clusters having the size of a few lattice constants.<sup>11,20</sup> The freezing temperature recorded at the point of noticeable increase of the width of the diffuse scattering peak has been found to be 100 K for a deuterated RADP ( $x=0.62$ ). Above 100 K the measurements<sup>20,21</sup> confirmed the quasielastic origin of these diffuse scattering peaks. Other experimental techniques, probing the system with different frequencies, have made possible the observation of the freezing temperature over 17 orders of magnitude in the frequency. This freezing is well described<sup>22,23</sup> phenomenologically by the Vogel-Fulcher<sup>24</sup> law which involves introducing a finite static freezing temperature.

The glass state is characterized by a distribution of relaxation times, which is broad in  $\ln\tau$  and spreads from

$10^{-12}$  sec to, perhaps, infinity. A given experimental technique is sensitive to those relaxation processes that are of the same order of magnitude as the characteristic time of measurements. Moreover, each technique measures a specific quantity. For example, incoherent neutron scattering is described by displacements of single atoms, while the dielectric measurements are sensitive to the local dipole moment made from correlated displacements of many particles. As a consequence, different experimental techniques measure different freezing temperatures. The broad distribution of relaxation times is often associated with the size of reorienting clusters.

The purpose of this work is to study the effects of the randomly competing interactions on the local motion of particles in a mixed system. In the pure crystal all particles behave indentially; sufficiently long-time averages are independent of particle location. In glasses the situation is different; local and interparticle potentials vary from site to site. Consequently, even at low temperatures no long range order can develop. In the strongly bonded regions of the glass, quasipermanent clusters are formed. At the same time, in the weakly bonded regions, the particles still perform motion, which gives rise to the observed relaxation times.

To study these phenomena the model from our previous paper,<sup>25</sup> hereafter denoted by I, will be used. The model considers the essential degrees of freedom of RDP, ADP, and RADP: the acid protons moving along the hydrogen bonds and the rubidium and ammonium particles moving along the axes of spontaneous polarization. The protons are situated in a local double-minimum potential and interact with neighboring particles. The model potential energy has the symmetry of a three-dimensional tetragonal phase. A layer of the glass or crystal that is perpendicular to the fourfold axes has been simulated by the molecular-dynamics method. Pa-

per I already contained the following results: the phase diagram, the temperature and concentration dependences of the glass order parameter, the dependence of the freezing temperature on the averaging time, the temperature dependence of the form and width of the diffuse scattering peaks at an incommensurate position, and the temperature dependence of the width of the quasielastic scattering described by the dynamic structure factor. To obtain reasonable results on the diffuse scattering we had to enlarge the simulated system in the scattering plane at the expense of the perpendicular direction.

In other models,<sup>26-28,15</sup> the acid-proton motion is approximated by the Ising spin variable  $S_{i,\mu} = \pm 1$  and the rubidium and ammonium ions are not considered explicitly. Our model can be reduced to the existing ones<sup>28,15</sup> by making the double-minimum potential infinitely deep and disregarding the motion of rubidium and ammonium. Basic interproton couplings in models<sup>28,15</sup> and paper I remain of the same form. Selke and Courtens<sup>28</sup> treated the ammonium-ion positions as additional random variables, and using the Monte Carlo method have found the phase diagram and glass order parameter of RADP. By replacing the ammonium variable by an additional effective random field between the acid protons and using the effective crystal approximation, Cowley *et al.*<sup>15</sup> have demonstrated the origin of incommensurate diffuse scattering peaks.

The paper is organized as follows. In Sec. II the details of the model and molecular-dynamics method are sketched. The relation between the ferroelectric and antiferroelectric clusters to the distribution of rubidium and ammonium is illustrated in Sec. III. Section IV deals with local displacement fluctuations in crystal and glass. The distribution of potential energies and the spectrum of relaxation times for crystal and glass are considered in Secs. V and VI, respectively.

## II. MODEL AND MOLECULAR-DYNAMICS METHOD

The model consists of unit cells labeled  $i,j$  with six particles in each unit cell: four protons  $\mu = 1,2,3,4$  and two particles  $\mu = 5,6$  representing combined  $\text{PO}_4$  and Rb or  $\text{PO}_4$  and  $\text{ND}_4$  groups. This model is shown in Fig. 1. Each particle has one degree of freedom, which is a displacement  $u_{i,j,\mu}$  from its average position. The protons  $\mu = 1,2$  and  $\mu = 3,4$  can move only along the  $y$  and  $x$  directions, respectively, in the model plane. These are the directions of the hydrogen bonds. The particles  $\mu = 5,6$  can move only along  $z$ , the direction normal to the model plane.

The potential energy  $V$  consists of a local potential,

$$A_{i,j,\mu} u_{i,j,\mu}^2 + G u_{i,j,\mu}^4, \quad (2.1a)$$

an interparticle potential between protons,

$$\begin{aligned} D_{i,j,6}(u_{i,j,1}u_{i,j,2} + u_{i,j,3}u_{i,j,4}) \\ + B_{i,j,6}(u_{i,j,1}u_{i,j,4} - u_{i,j,2}u_{i,j,3}) \\ + P u_{i,j,1}u_{i,j,2'}, \end{aligned} \quad (2.1b)$$

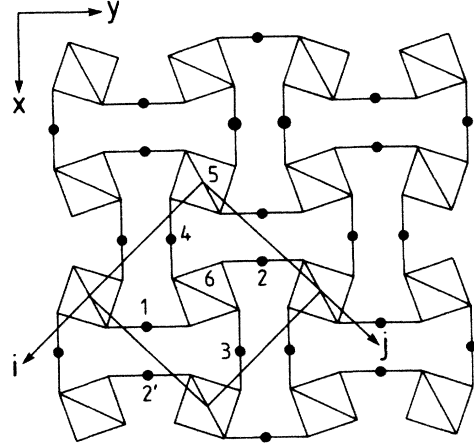


FIG. 1. Model used in the molecular-dynamics simulation. This is a projection of the structure RADP down the  $c$  axis. The unit cell contains four protons, 1, 2, 3, and 4. Two combined Rb and  $\text{PO}_4$  or  $\text{NH}_4$  and  $\text{PO}_4$  particles, 5 and 6, are shown by the large squares.

an interparticle potential between protons and rubidium or ammonium,

$$C u_{i,j,6}(u_{i,j,1} - u_{i,j,2} + u_{i,j,3} - u_{i,j,4}), \quad (2.1c)$$

the interparticle potential between the rubidium or ammonium particles,

$$-E u_{i,j,5}u_{i,j,6}, \quad (2.1d)$$

and similarly for other particles. The local springs  $A_{i,j,\mu}$  are different for protons between two rubidium and two ammonium particles. For rubidium-ammonium neighbors, an average is taken. The constants  $D_{i,j,\mu}$  and  $B_{i,j,\mu}$  depend on the kind of particle located at the site  $\mu = 5$  or  $6$ . A complete form of the potential energy has been given in paper I, Eqs. (3.1)–(3.5), hereafter abbreviated as Eqs. (I.3.1)–(I.3.5). Two sets of parameters quoted in Table I of paper I have been used, one corresponding to the model of RDP and the other to the model of ADP. The parameter sets promote the phase transitions from paraelectric to ferroelectric and antiferroelectric phases, respectively, with condensation of the modes with correct wave vectors and correct irreducible representations.

In the glass model the rubidium and ammonium particles are distributed randomly among  $\mu = 5,6$  sites with a concentration  $x = 0.62$ . The coupling constants at a given place have been taken from Table I of paper I in accordance with the local distribution of particles.

The system used in the computer simulation was a square two-dimensional crystallite of the size of  $38 \times 38$  unit cells. In total the system consisted of  $N_0 = 8741$  particles. Free-boundary conditions and the microcanonical ensemble were used. The Newton equations of motion were solved by a simple difference scheme. The iteration step was  $\Delta t = 0.05\tau_0$ , where  $\tau = 2\pi/\omega_0$  is the

characteristic mode frequency. The temperature was described by the average kinetic energy. The system was cooled or heated by a delicate change of particle velocities in each iteration step. We have calculated averages  $\langle O \rangle_\tau$  of dynamical variables  $O$  over a long but finite time  $\tau$ .

The models of RDP and ADP crystals exhibit phase transitions from paraelectric to ferroelectric and to antiferroelectric phases at temperatures  $T_c = 0.00565$  and  $T_c = 0.00430$ , respectively. The RDP transition is driven by an order parameter at the zone center, while ADP is the result of the condensation of an irreducible representation at the zone boundary. The RDP and ADP can exist in two and four domains, respectively.

The glassy state of the model has been characterized by the glass Edwards-Anderson order parameter

$$\eta_\tau = \frac{1}{N_0} \sum_{i,j,\mu} \langle \langle u_{i,j,\mu} \rangle_\tau \rangle^2, \quad (2.2)$$

where the summation runs over all particles. The  $\eta_\tau$  does not vanish if at least a few particles remain either in positive or negative positions during time  $\tau$ . The freezing temperature has been defined by extrapolating the temperature-dependent  $\eta_\tau$  curve monotonously to zero. The freezing temperature  $T_f(\tau)$  depends on the averaging time  $\tau$ . For averaging time  $\tau = 100\tau_0$  and  $10000\tau_0$ , the freezing temperatures have been  $T_f = 0.00425$  and  $0.00270$ , respectively. At infinite averaging time one expects the lowest possible freezing temperature, the so-called static freezing temperature  $T_0 = T_f(\tau = \infty)$ . Computer simulation does not allow us to study this.

### III. FERROELECTRIC AND ANTIFERROELECTRIC CLUSTERS

In the glass, below the freezing temperature, one may expect chemical clusters of rubidium and ammonium to promote the appearance of the ferroelectric and antiferroelectric proton clusters, respectively. To verify that statement, the glass system was twice cooled slowly to the temperature  $T = 0.00100$ , which is much lower than  $T_f$ . Then it was equilibrated and the position of each proton was averaged over  $100\tau_0$ . The two runs were performed with the same initial and final temperatures, the same distribution of rubidium and ammonium, and the same cooling rate and equilibration times. The energies of the low-temperature states also proved to be the same. However, the two runs differed in the distribution of initial velocities and initial positions of particles.

As a result of those runs, two maps of average proton positions were obtained. Knowing the elementary ferroelectric and antiferroelectric patterns of proton displacements, we assigned the type of cluster (ferroelectric or antiferroelectric) and its orientation to the configurations of protons. The result of this procedure is shown in Fig. 2. According to the symmetry reduction in the phase transitions of RDP and ADP, the ferroelectric and antiferroelectric domains can exist in two and four (including two antiphase) orientations, respec-

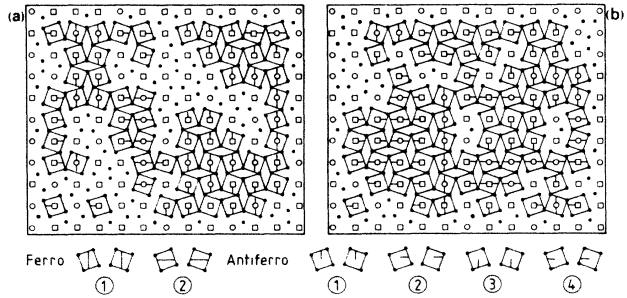


FIG. 2. Cluster structure of two runs, obtained as a result of independent cooling processes. The rubidium ( $\circ$ ) and ammonium ( $\square$ ) particles are indicated. The notations for the ferroelectric and antiferroelectric clusters together with their orientations are shown at the bottom of the figure.

tively. Hence, each cluster has a definite domain orientation.

Figure 2 allows us to draw the following conclusions. (i) There are regions where the assignment of the type of cluster is not possible. (ii) The ferroelectric or antiferroelectric clusters occur in regions of rubidium or ammonium chemical clusters, respectively. Thus, chemical clusters promote corresponding clusters of protons. (iii) The orientations of ferroelectric or antiferroelectric clusters are random and, generally, different on both maps.

The maps are history dependent. Cooled twice from the paraelectric phase, the glass approaches two different patterns of cluster orientations. In the phase space the two patterns correspond to two different local minima.

### IV. LOCAL DISPLACEMENT FLUCTUATIONS

In the simulation we can try to localize regions where protons do not jump over local barriers, regions where they undergo an active motion. A suitable quantity that can serve as a measure of local activity of particles is the squared displacement fluctuation (SDF)

$$W_{i,j,\mu} = \langle u_{i,j,\mu}^2 \rangle_\tau - \langle u_{i,j,\mu} \rangle_\tau^2, \quad (4.1)$$

where  $\tau$  is a finite averaging time. If a particle remains in one of the local minima during time  $\tau$  its SDF is small. If a particle is visiting both minima in a comparable time then its SDF becomes large.

Below we show a few maps of SDF. They all represent the central part of  $14 \times 14$  unit cells of the system, which contain 30% of particles. The distribution of rubidium and ammonium was fixed in the calculations. The symbols given on the maps, Figs. 3–6, represent the particles. The size of each symbol is proportional to the value of SDF, Eq. (4.1). Each map in each figure was obtained from the same initial equilibrated state but averaged over different times  $\tau$ .

#### A. Glass model of RADP

Figure 3 shows subsequent maps at averaging times  $100\tau_0$ ,  $500\tau_0$ ,  $2500\tau_0$ , and  $12500\tau_0$  and low temperature  $T = 0.00103$ . The freezing temperatures are  $0.00425$ ,

0.003 70, 0.003 16, and 0.002 60, respectively. As seen in Fig. 3, in spite of such a low temperature, some particles jump between the minima. For the short time  $100\tau_0$  the number of active particles is small, but for the longest time  $12\,500\tau_0$  it becomes larger. There are particles or small clusters which are always active. Other clusters are present in some of the maps only. For particles belonging to such clusters one should assume active motion during some time, followed by quiet periods. Apart from that, one can easily notice large frozen regions of quasipermanent clusters. It was also found that during the time of  $12\,500\tau_0$ , 52% of the protons have not jumped even once to the opposite local minimum. The remaining particles have performed on the average 100 jumps during the observed period of time. Hence, well-localized regions of activity are identified.

At the higher temperatures 0.002 04 and 0.003 04, as shown in Fig. 4, one is still able to recognize frozen regions. For  $T=0.003\,04$  and  $2500\tau_0$  the regions of quasipermanent clusters have shrunk, as expected for conditions close to the freezing temperature. The maps obtained well above the freezing temperature showed a homogeneous distribution of SDF.

Different protons exhibit different SDF amplitudes. The distribution of these amplitudes can be described as

$$p(W) = \frac{1}{N} \sum_{\substack{i,j,\mu \\ W < W_{i,j,\mu} < W + dW}} 1, \quad (4.2)$$

where the summation runs only over those protons whose SDF amplitudes are confined to the interval

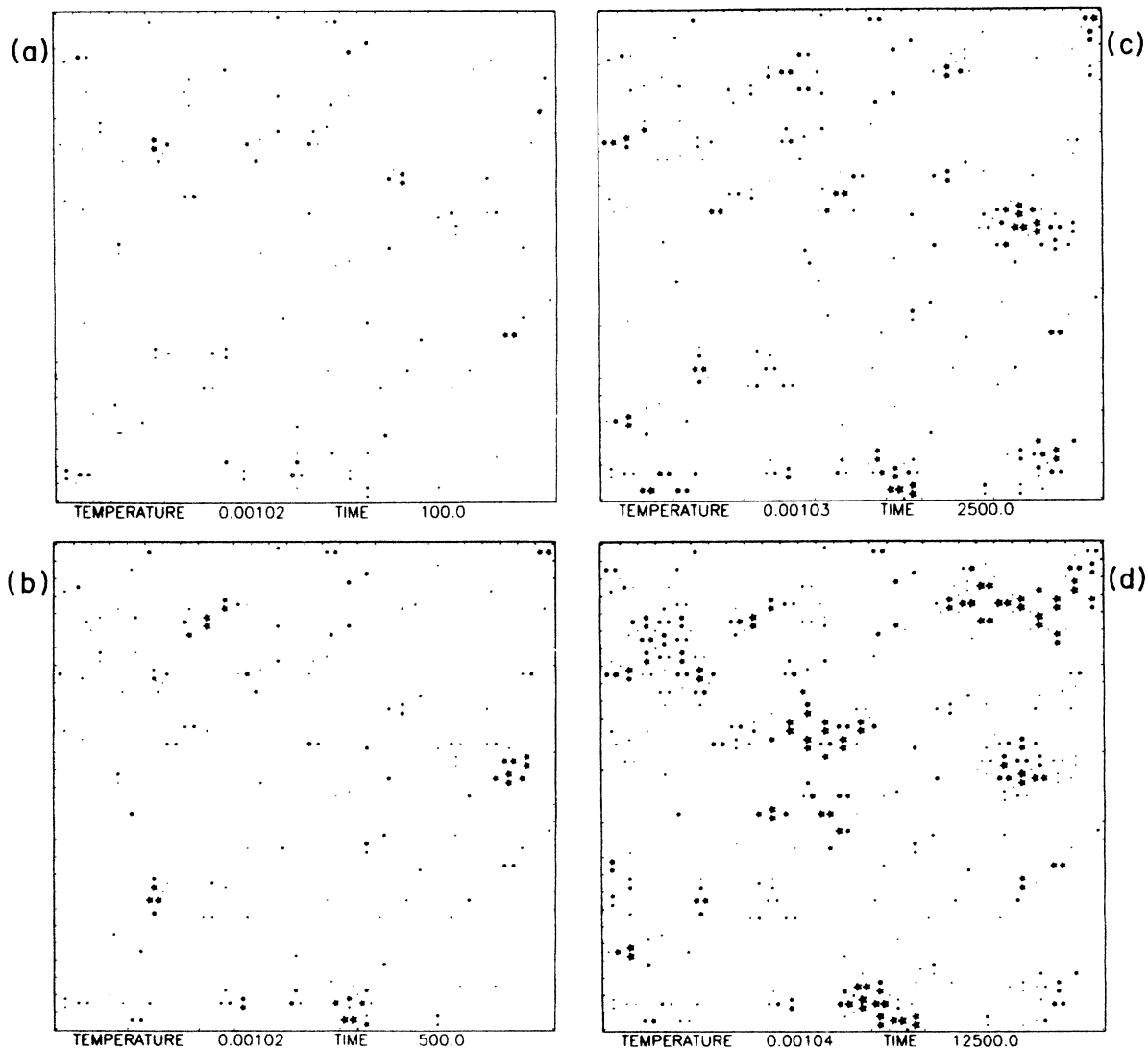


FIG. 3. Maps of the squared displacement fluctuations for a glassy state, Eq. (4.1), obtained at a temperature  $T=0.001\,03$ . (a)–(d) correspond to the averaging times  $100\tau_0$ ,  $500\tau_0$ ,  $2500\tau_0$ , and  $12\,500\tau_0$ , respectively.

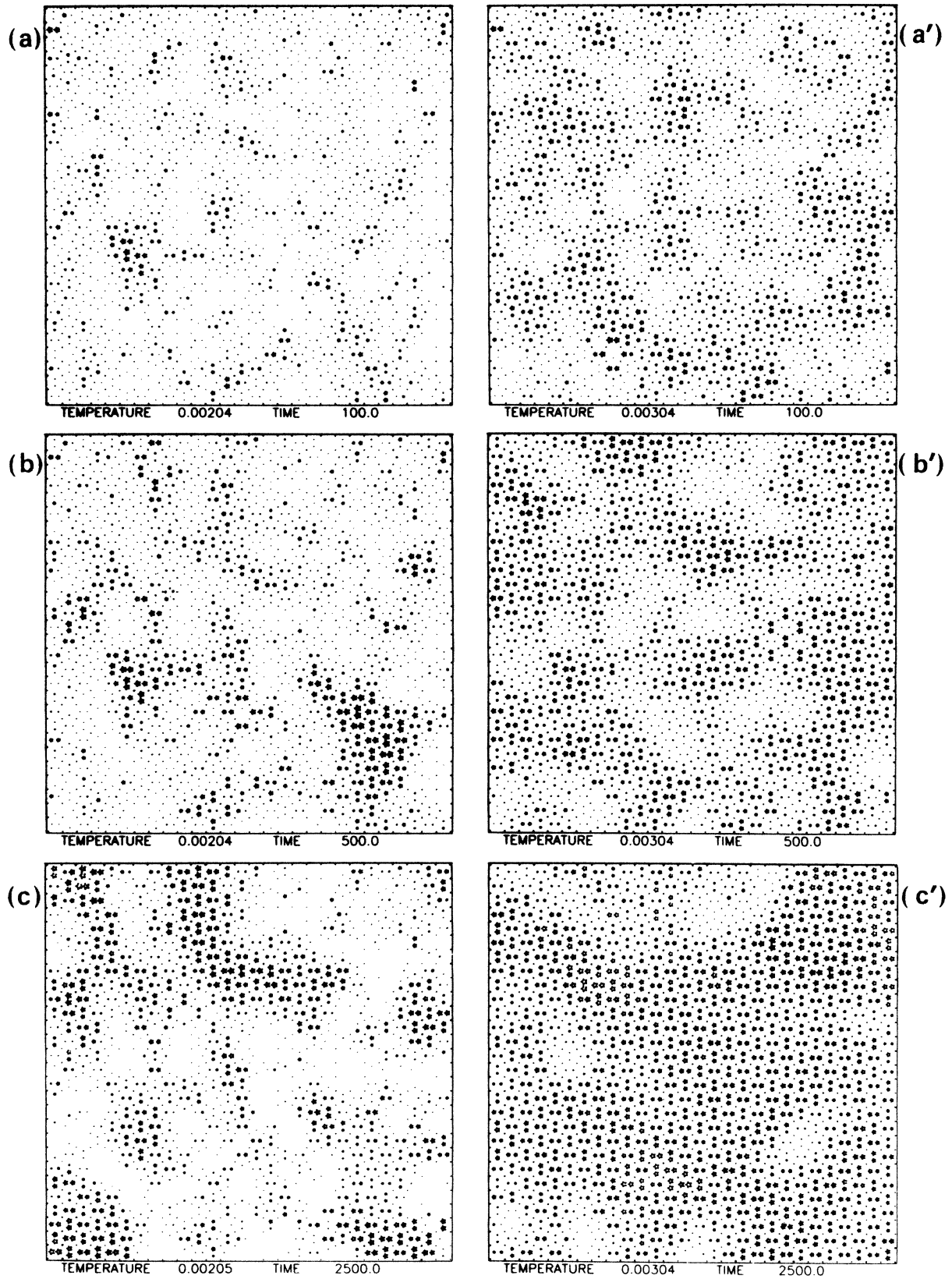


FIG. 4. Maps of the squared displacement fluctuations for a glassy state, Eq. (4.1). (a)–(c) are obtained at temperature  $T=0.00204$ , (a')–(c') are maps obtained at temperature  $T=0.00304$ . The corresponding averaging times are (a),(a'),  $100\tau_0$ ; (b),(b'),  $500\tau_0$ ; (c),(c'),  $2500\tau_0$ .

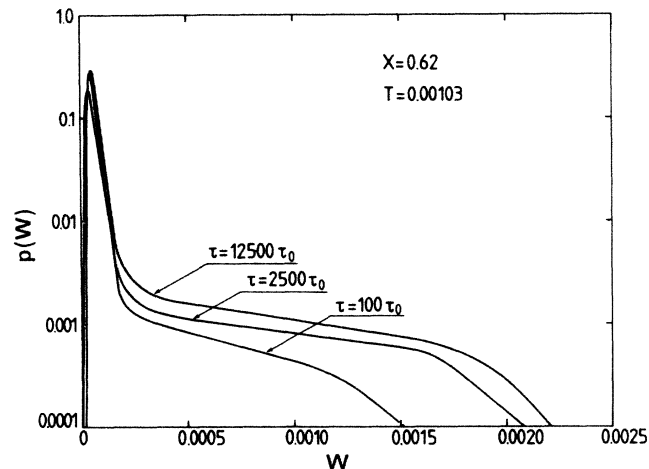


FIG. 5. Distribution  $p(W)$ , Eq. (4.2), of the squared displacement fluctuations in a glassy state for some averaging times  $\tau$ .

( $W, W + dW$ ), and  $N$  is the number of protons. Figure 5 shows the  $p(W)$  distributions at  $T=0.00103$  for three averaging times. The distributions have been obtained during the same runs as the respective maps of Fig. 3. As seen in Fig. 5, a majority of particles, oscillating within one minimum, possess small SDF amplitudes. The other particles have amplitudes that correspond to the jump motion between local minima. For longer averaging times, more particles join the jumping group.

Figure 6 represents the distribution of SDF amplitudes calculated for various temperatures. As expected, above the freezing temperature  $T_f=0.00316$  for  $\tau=2500\tau_0$ , the distribution  $p(W)$  shows one peak at the squared half-distance between local minima. The peaks

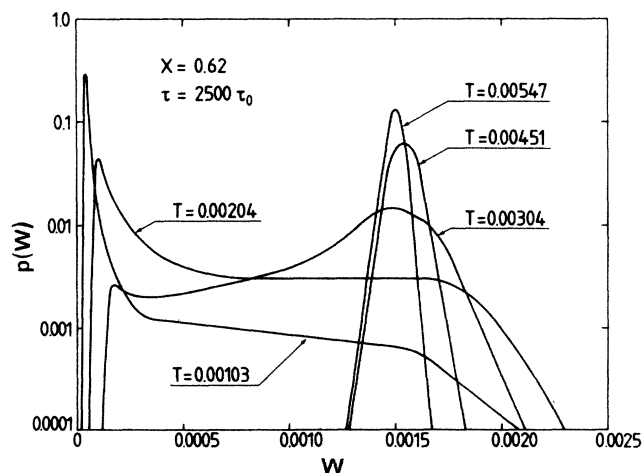


FIG. 6. Distribution  $p(W)$ , Eq. (4.2), of the squared displacement fluctuations in glassy and paraelectric states. For the averaging time  $\tau=2500\tau_0$ , the freezing temperature is  $T_f=0.00316$ .

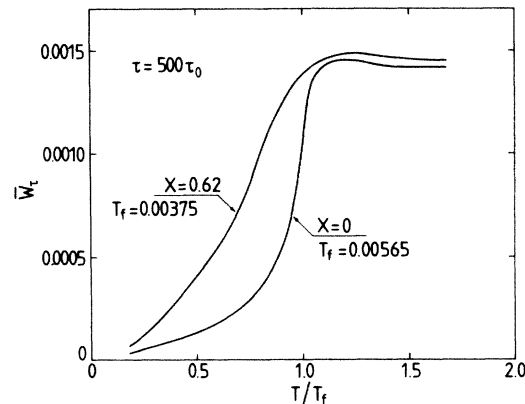


FIG. 7. First moment of the square displacement fluctuations, Eq. (4.3), for glassy and crystal RDP states as a function of reduced temperatures.

have a tendency to become narrower with increasing temperature. Below  $T_f$  the distribution  $p(W)$  becomes fairly broad. Protons belonging to quasipermanent clusters contribute to the peak of the  $p(W)$  spectrum at small values. The jumping particles produce a wide plateau.

We also calculated the first moment, or the average SDF,

$$\bar{W}_\tau = \int_0^\infty W p(W) dW. \quad (4.3)$$

It is presented as a function of the reduced temperature in Fig. 7. This average increases with temperature until the freezing temperature is reached. Above  $T_f$  all protons jump between both local minima frequently, and thus  $\bar{W}_\tau$  remains constant.

## B. Crystal model of RDP

Figure 8 shows four maps of the SDF for a pure crystal model of RDP at a temperature close to the phase transition  $T_c=0.00565$ . For the short-time average of  $20\tau_0$  the clusters of larger displacements are dynamical critical fluctuations. For the long-time averages the map becomes more homogeneous, since all the particles located at identical potentials behave similarly. Any excitation easily propagates through the crystal and therefore the motion is not localized.

The quantitative description of this effect is given in Fig. 9, where the distribution of SDF amplitudes is presented. This should be compared with Fig. 6 showing the strikingly different SDF distribution for glass at low temperature. At  $T=0.00306$  some jumps have occurred, but the jump process has not been localized. The localization would cause a long tail for large  $W$  values. The broad distribution at  $T=0.00543$  reflects the critical fluctuations which are so slow that the time  $2500\tau_0$  cannot serve as a representative average. Above the phase transition all protons jump between local minima with the same rate, producing a single peak at the same position as for the high-temperature glass system.

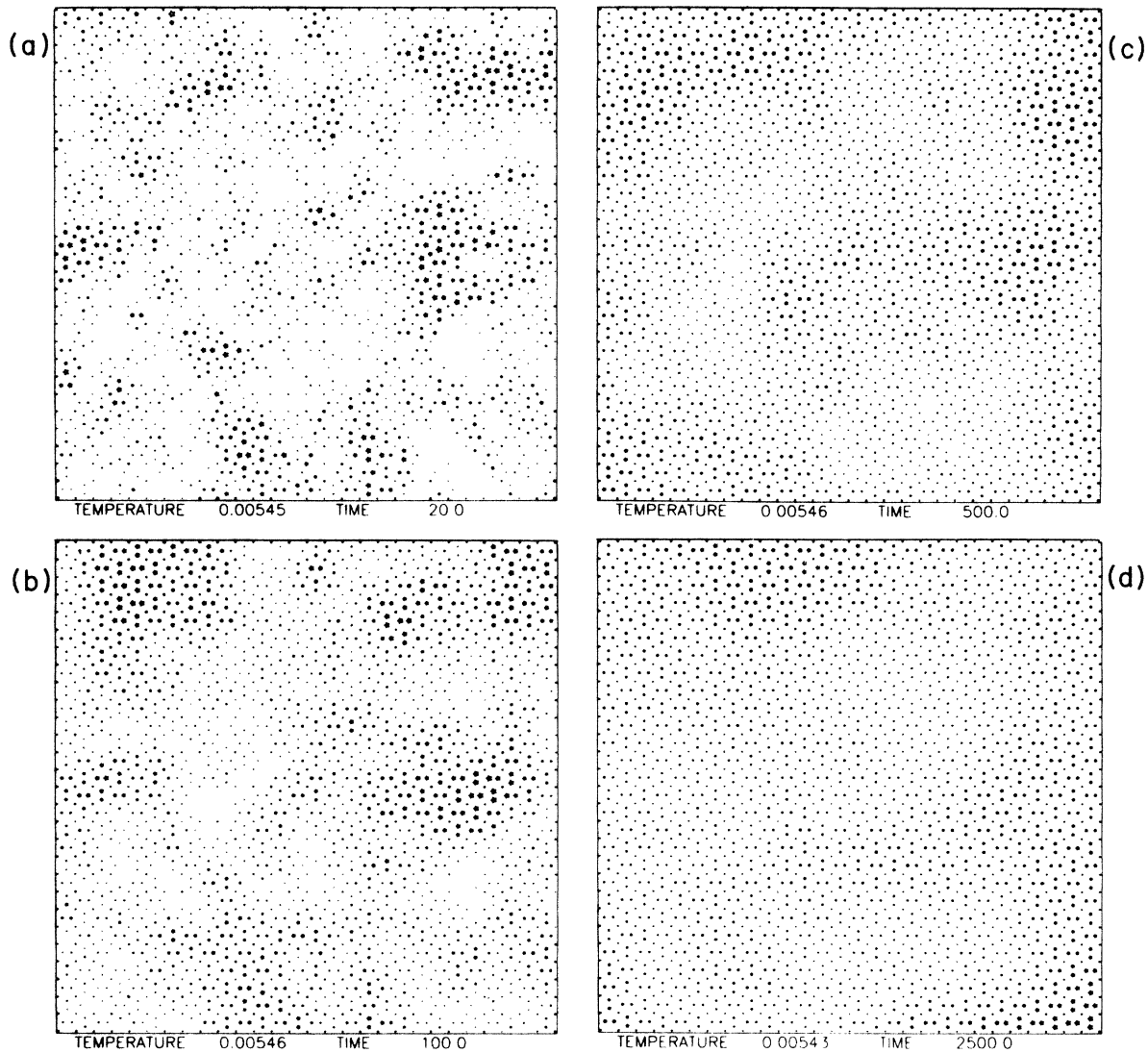


FIG. 8. Maps of the squared displacement fluctuations for the crystal RDP, Eq. (4.1), obtained at temperatures  $T=0.00545$  close to the critical temperature  $T_c=0.00565$ . (a)–(d) correspond to the averaging times  $20\tau_0$ ,  $100\tau_0$ ,  $500\tau_0$ , and  $2500\tau_0$ , respectively. The size of symbols on all the maps is not rescaled and therefore they are comparable.

The average SDF, Eq. (4.3), calculated from the distribution  $p(W)$  in Fig. 9, is shown in Fig. 7 together with a similar curve for the glass system. The increase of the average SDF for the pure crystal occurs in the critical region and is confined to a narrow interval of temperatures. In the glass system that region is much broader.

The above effect has been confirmed experimentally. The incoherent inelastic neutron scattering is proportional to the SDF. In Fig. 10 inelastic incoherent neutron scattering measurements at the constant energy transfer for the structural glass  $\text{Rb}_{0.65}(\text{NH}_4)_{0.35}\text{H}_2\text{AsO}_4$  (Ref. 29) and crystalline  $\text{RbH}_2\text{AsO}_4$  samples are compared. The results are analogous to the curves of Fig. 7.

## V. DISTRIBUTION OF PROTON POTENTIAL ENERGIES

The potential energy of the system, Eqs. (I.3.1)–(I.3.5), can be written as a sum over potential energies of individual particles,

$$V = \frac{1}{N_0} \sum_{i,j,\mu} Y_{i,j,\mu}. \quad (5.1)$$

We have introduced a deviation of the individual average potential

$$V_{i,j,\mu} = \langle Y_{i,j,\mu} \rangle_\tau - \langle V \rangle_\tau, \quad (5.2)$$

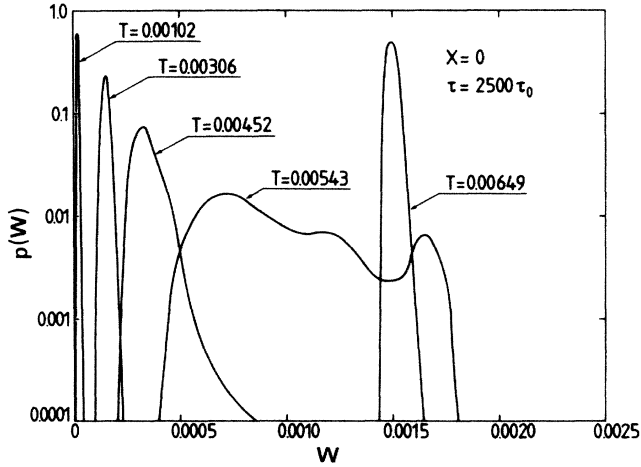


FIG. 9. The distribution  $p(W)$ , Eq. (4.2), of the squared displacement fluctuations for the crystal RDP in ferroelectric and paraelectric states ( $T_c = 0.00565$ ).

where  $\langle V \rangle_\tau$  is the average potential of the whole crystal, per particle. Its temperature dependence is given in Fig. 4 of I. Similarly to the distribution of SDF's, Eq. (4.2), the distribution of local potential-energy deviations for protons

$$p(V) = \frac{1}{N} \sum_{V < V_{i,j,\mu} < V+dV} 1 \quad (5.3)$$

were calculated for the RDP crystal and for the glass system. The results are displayed in Figs. 11 and 12, respectively. The averaging time used was  $\tau = 2500\tau_0$ .

In our model the potential energies of rubidium and ammonium at the minimum of the local single minimum potentials and the potential energies of protons at the top of the local potential barriers are zero. Hence, fluctuations of rubidium and ammonium give positive contributions to the average potential energy  $\langle V \rangle_\tau$  while

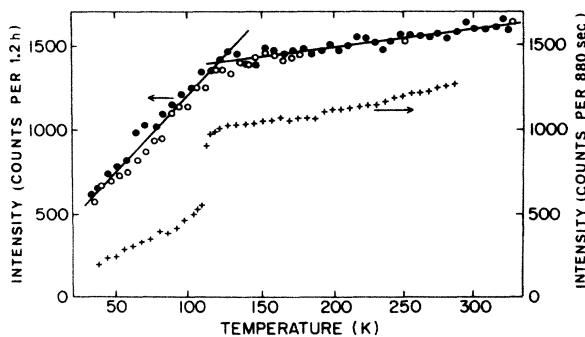


FIG. 10. Comparison of the incoherent inelastic neutron scattering at constant energy transfer of  $-0.5$  THz for the mixture  $\text{Rb}_{0.65}(\text{NH}_4)_{0.35}\text{H}_2\text{PO}_4$  (Ref. 29) (+) and pure  $\text{RbH}_2\text{AsO}_4$  (O, ●).

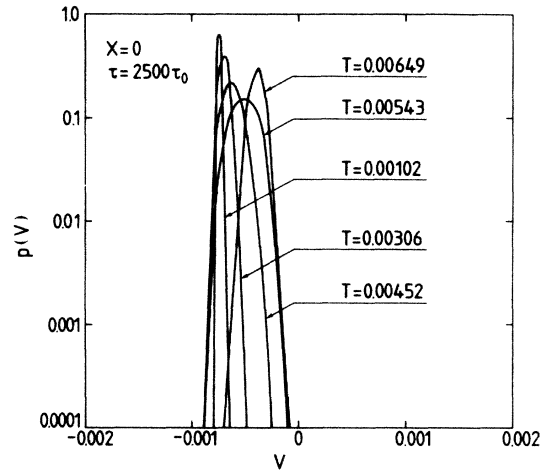


FIG. 11. Distribution of individual potential energy deviations for protons, Eq. (5.3), in a crystalline phase of RDP.

negative contributions to  $\langle V \rangle_\tau$  are expected from protons residing in one of the local minima. In agreement with Eq. (5.2), the two factors shift the potential energies of protons  $V_{i,j,\mu}$ , and the distribution  $p(V)$ , towards negative values of  $V$ .

In the RDP crystal, the distribution  $p(V)$  is narrow, as shown in Fig. 11. The protons are subject to identical potentials, and therefore the width of the distribution is attributed to the finiteness of the averaging process, which is less sufficient closer to the critical temperature. Therefore, at  $T=0.00543$  the width of the  $p(V)$  distribution is the largest. Increasing the temperature, the protons reside for a longer time on the local barriers, diminishing the difference between the potential energies. Hence, the average position of the peaks in Fig. 11 increases with the temperature.

In the glassy state at low temperatures, as shown in Fig. 12, one observes a dramatic broadening due to the

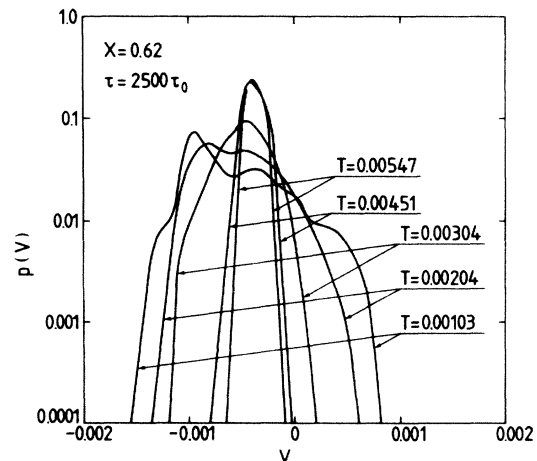


FIG. 12. Distribution of individual potential-energy deviations for protons, Eq. (5.3), in a glassy state.



distribution of local minima for protons and to the variety of the interparticle potentials. Indeed, the potential energies of ferroelectric and antiferroelectric clusters are different (see Fig. 4 of I). Moreover, the minima of the local potentials of protons, those between two rubidia or two ammonia, are different. All these states generate at low temperatures a large distribution of the proton potential energies. Above the freezing temperature, where quasipermanent clusters vanish, all particles explore the region of potential energy close to zero, and the distribution becomes narrower and resembles the crystal case.

## VI. SPECTRUM OF RELAXATION TIMES

In spin glasses and structural glasses the dynamics play a major role in the freezing process. The conventional freezing temperature  $T_f(\tau)$  is defined by the point where the Edwards-Anderson order parameter, Eq. (2.2), averaged over time  $\tau$  tends to zero. Below  $T_f$  an intensive motion in the system is still present. This motion dies out in the course of temperature decrease. It is believed that there exists a "static" freezing temperature  $T_0 = T_f(\tau = \infty)$  described by an infinite averaging time below which the frozen-in clusters of infinite surface<sup>30</sup> exist. The averaging time  $\tau$  and the associated freezing temperature  $T_f$  can be related to each other by the phenomenological Vogel-Fulcher<sup>24</sup> law, which is applicable to RADP.<sup>22</sup> Other relationships have also been proposed.<sup>31,32</sup>

In glasses, the relaxation times form a broad spectrum ranging from extremely short times on the order of  $10^{-12}$  sec to some finite cutoff time. At a given freezing temperature  $T_f(\tau)$ , the cutoff time is of the same order as the respective averaging time  $\tau$ .

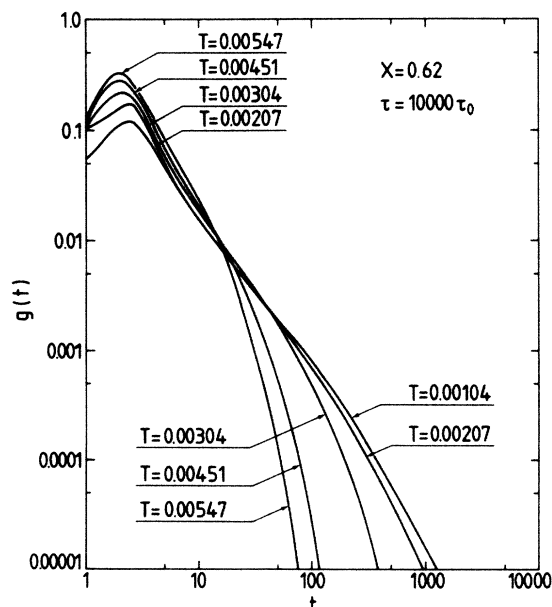


FIG. 13. Log-log plot of the distribution  $g(t)$  of elementary relaxation times of protons for the glassy state.

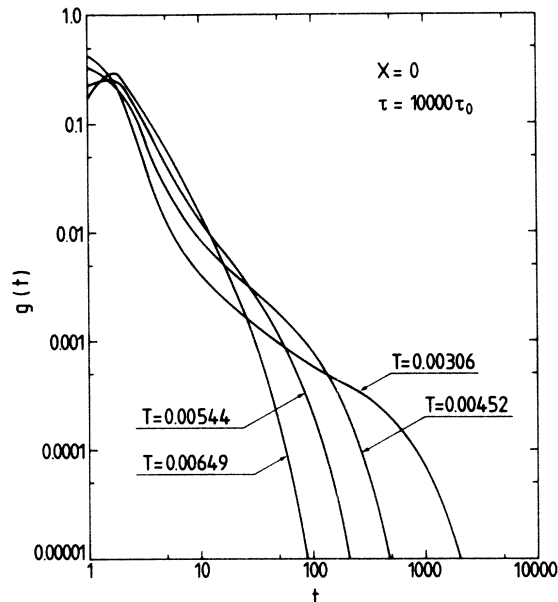


FIG. 14. Log-log plot of the distribution  $g(t)$  of elementary relaxation times of protons for the crystalline phase of RADP.

To whatever quantity the relaxation time is related, the elementary relaxation step will be the jump of protons between the local minima. Simplifying the problem a little, one can easily calculate the distribution of elementary relaxation times using the following procedure: We define that a particle  $(i, j, \mu)$  has jumped from one local minimum to another when the displacement  $u_{i,j,\mu}(t)$  alternates sign between two subsequent iteration steps  $\Delta t$ . Thus, according to our definition, the jump occurs if the product

$$u_{i,j,\mu}(n \Delta t) u_{i,j,\mu}[(n-1) \Delta t] \quad (6.1)$$

becomes negative. The time between two subsequent jumps of the same particle defines the elementary relaxation time.

The elementary relaxation times of all protons, except those located in the unit cells at the border of the system, have been segregated into a histogram representing a distribution of the relaxation times  $g(t)$ . Figures 13 and 14 show the resulting distributions for the glass RADP and pure RADP systems, respectively, as a function of temperature. Each distribution is a result of a run which lasted  $10\,000\tau_0$ . The distributions have been normalized

$$\int_0^{\infty} g(t) dt = 1;$$

therefore, they do not reflect the total number of jumps.

### A. Glass model of RADP

Above  $T_f$ , the presence of quick proton jumps involve a narrow spectrum of  $g(t)$  peaked at short relaxation times, as shown in Fig. 13. Below  $T_f$ , the spectrum evolves towards longer relaxation times at the expense of

the short times. Protons from active regions of the glass contribute to the short relaxation times while protons of quasipermanent clusters give rise to the long relaxation times.

Above  $1000\tau_0$  the elementary relaxation times have not been recorded because the time of the simulation was finite and the system was of a small size. Large fluctuations cannot appear in the small system, thus large clusters are not able to reorient.

A wide spectrum of experimentally observed relaxation times of RADP have been constructed<sup>22</sup> from the neutron, Raman, Brillouin, and dielectric measurements. However, each experimental technique deals with other quantity. The incoherent neutron scattering is defined by the single-atom motion and hence by the distribution of the elementary relaxation times. For times longer than  $10^{-8}$  sec, the dielectric measurements are usually used. Such measurements are sensitive not to the distribution of the relaxation times of single protons but to the corresponding distribution of the local dipole moments of the ferroelectric clusters. Such clusters reorient rarely so they cannot contribute significantly to the distribution of the elementary relaxation times. We add that on the series of maps of proton configurations the reorientation of clusters of a size of one, two lattice constants has been observed.

The result fits the concept of hierarchically constrained dynamics<sup>33</sup> that involves a hierarchy of degrees of freedom, from fast to slow. The fastest degrees of freedom involve single atoms or very small clusters, and distributions of their elementary relaxation times have been recorded in Fig. 13. Larger groups of atoms or even quasipermanent clusters are only able to move when several of the fastest atoms happen to move in the right way, weakening the constraints at the cluster boundary and promoting the reorientation of the cluster.

At low temperatures it is expected that not all protons jump. Using Eq. (6.1),  $n$ —the number of protons which have been jumped at least once—was recorded and the result of the ratio  $n/N$  shown in Fig. 15. In spite of a long-time average of  $\tau = 10\,000\tau_0$ , many protons have not jumped even once below  $T \approx 0.002\,00$ .

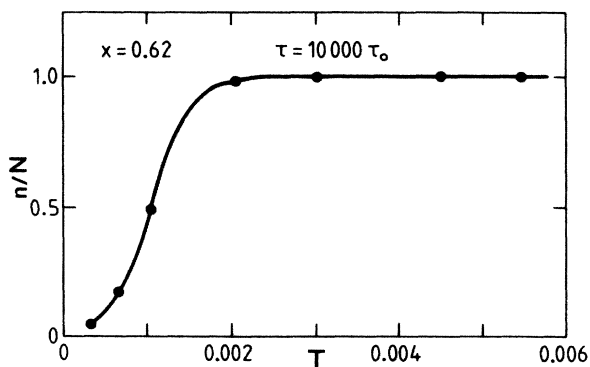


FIG. 15. Temperature dependence of relative number of particles  $n/N$  in a glassy state which during the time  $10\,000\tau_0$  have performed at least one jump over the local barrier.

## B. Crystal model of RDP

Above  $T_c$ , the spectrum of the elementary relaxation times of the crystal, as shown in Fig. 14, is similar to the corresponding spectrum of the glass. Below  $T_c$ , and at the same reduced temperatures, the rate of proton jumps is considerably lower in the crystal than in the glass. In the ferroelectric phase, two types of domains separated by the domain walls are formed. There, the jump motion of protons organizes into a collective motion of a domain wall. The oscillations of the domain wall involve fast jump motion of these protons which are located in it. These protons contribute to that part of  $g(t)$  which corresponds to the short relaxation times.

The spectra at  $T = 0.003\,06$  and  $0.004\,52$  exhibit, in addition, a remarkable increase of  $g(t)$  at the long relaxation times. These parts of the spectra convert in another representation of the spectrum  $G(t)$ , where  $G(t) = \int_0^t g(t) dt$ , into the maxima placed at longer relaxation times  $500\tau_0$  and  $50\tau_0$ , respectively. The maxima arise because the domain wall propagates and returns to the same protons after longer periods. The domain wall ceases to propagate below  $T = 0.002\,00$ . Of course, within domains are protons which jump owing to the activation energies and they contribute also to the spectrum of the elementary relaxation times.

## VII. SUMMARY

From the computer simulation and the analysis of the configurational maps the following picture of RADP glass emerges. In high temperatures the glass behaves much like paraelectric crystal. On cooling, the chemical clusters of rubidium and ammonium, of the size of a few lattice constants, promote the formation of quasipermanent ferroelectric or antiferroelectric clusters of protons, respectively. The orientation of the clusters is of either one of two ferroelectric or one of four antiferroelectric crystal domains, respectively. These orientations are random; they depend on sample history and freeze gradually during the cooling process. Moreover, the clusters of given orientations may be subject to constraints superimposed by the surrounding quasipermanent clusters of other orientations. The quasipermanent clusters contribute to the glass order parameter and to the elastic coherent diffuse scattering.

In the intermediate region between the quasipermanent clusters, mainly in the region of competing interaction potentials, the protons are active and jump frequently over local barriers.

The local kinetic and potential energies of the glass fluctuate. Such a local fluctuation travels in the system, and in the active region is manifest in the motion of the jumping protons. If the excess of energy travels away from the active region, the proton remains in one of the local minima. Hence, a single proton jumps irregularly; active periods are interrupted by quiet intervals.

Entering a quasipermanent cluster, an energy fluctuation is converted into a phonon-type motion. Rare jumps of protons, expected to be even collective, are initiated by active regions attached to cluster boundaries. The

collective jumps may lead to a reorientation of the quasi-permanent cluster and may influence the macroscopic quantities, such as net polarization. These events, no matter how seldom, contribute to the longer relaxation times.

#### ACKNOWLEDGMENTS

The authors wish to thank H. Stiller, U. Buchenau, and E. Courtens for fruitful discussions and valuable comments.

- 
- <sup>1</sup>E. Courtens, Phys. Rev. Lett. **52**, 69 (1984).  
<sup>2</sup>E. Courtens, Phys. Rev. B **33**, 2975 (1986).  
<sup>3</sup>V. H. Schmidt, S. Waplak, S. Hutton, and P. Schnackenberg, Phys. Rev. B **30**, 2795 (1984).  
<sup>4</sup>G. A. Samara and H. Terauchi, Phys. Rev. Lett. **59**, 347 (1987).  
<sup>5</sup>E. Courtens and H. Vogt, J. Chim. Phys. **82**, 317 (1985).  
<sup>6</sup>E. Courtens, F. Huard, and R. Vacher, Phys. Rev. Lett. **55**, 722 (1985).  
<sup>7</sup>E. Courtens, R. Vacher, and Y. Dagorn, Phys. Rev. B **33**, 7625 (1986).  
<sup>8</sup>E. Courtens, R. Vacher, and Y. Dagorn, Phys. Rev. B **36**, 318 (1987).  
<sup>9</sup>E. Courtens and R. Vacher, Phys. Rev. B **35**, 7271 (1985).  
<sup>10</sup>S. Iida and H. Terauchi, J. Phys. Soc. Jpn. **52**, 4044 (1983).  
<sup>11</sup>E. Courtens, T. F. Rosenbaum, S. E. Nagler, and P. M. Horn, Phys. Rev. B **29**, 515 (1984).  
<sup>12</sup>H. Terauchi, T. Futamura, Y. Nishihata, and S. Iida, J. Phys. Soc. Jpn. **53**, 483 (1985).  
<sup>13</sup>S. Hayase, T. Futurama, H. Sakshita, and H. Terauchi, J. Phys. Soc. Jpn. **54**, 812 (1985).  
<sup>14</sup>R. A. Cowley, T. Ryan, and E. Courtens, J. Phys. C **18**, 2793 (1985).  
<sup>15</sup>R. A. Cowley, T. Ryan, and E. Courtens, Z. Phys. B **65**, 181 (1986).  
<sup>16</sup>S. Amin, R. A. Cowley, and E. Courtens, Z. Phys. B **67**, 229 (1987).  
<sup>17</sup>J. Slak, R. Kind, R. Blinc, E. Courtens, and S. Žumer, Phys. Rev. B **30**, 85 (1984).  
<sup>18</sup>R. Blinc, D. C. Ailon, B. Gunther, and S. Žumer, Phys. Rev. Lett. **57**, 2826 (1986).  
<sup>19</sup>E. Courtens, J. Phys. (Paris) Lett. **43**, L199 (1982).  
<sup>20</sup>H. Grimm, K. Parlinski, W. Schweika, E. Courtens, and H. Arend, Phys. Rev. B **33**, 4963 (1986).  
<sup>21</sup>H. Grim and J. Martinez, Z. Phys. B **64**, 13 (1986).  
<sup>22</sup>E. Courtens and H. Vogt, Z. Phys. B **62**, 143 (1986).  
<sup>23</sup>E. Courtens, Jpn. J. Appl. Phys. Suppl. **24-2**, 70 (1985).  
<sup>24</sup>H. Vogel, Z. Phys. **22**, 645 (1921); G. S. Fulcher, J. Am. Ceram. Soc. **8**, 339 (1925).  
<sup>25</sup>K. Parlinski and H. Grimm, Phys. Rev. B **33**, 4868 (1986), denoted paper I in the text.  
<sup>26</sup>P. Prelovšek and R. Blinc, J. Phys. C **15**, L985 (1982).  
<sup>27</sup>E. Matsushita and T. Matsubara, Prog. Theor. Phys. **71**, 235 (1984); J. Phys. Soc. Jpn. **54**, 1161 (1985); **54**, 2032 (1985); **55**, 666 (1986).  
<sup>28</sup>W. Selke and E. Courtens, Ferroelectr. Lett. **5**, 173 (1986).  
<sup>29</sup>H. Grimm and J. Slak, Phys. Status Solidi B **137**, K37 (1986).  
<sup>30</sup>M. Cyrot, Phys. Lett. **83A**, 275 (1981).  
<sup>31</sup>K. Binder and A. P. Young, Phys. Rev. B **29**, 2864 (1984).  
<sup>32</sup>K. Binder and W. Kinzel, in *Disordered Systems and Localization*, Vol. 149 of *Lecture Notes in Physics*, edited by C. Castellani, C. Di Castro, and L. Peliti (Springer-Verlag, Berlin, 1981), p. 124.  
<sup>33</sup>R. G. Palmer, D. L. Stein, E. Abrahams, and P. W. Anderson, Phys. Rev. Lett. **53**, 958 (1984).